JOURNAL OF CATALYSIS **178,** 174–181 (1998)
ARTICLE NO. CA982107

n-Hexane Reforming Reactions over Basic Pt-ETS-10 and Pt-ETAS-10

Andreas Philippou,* Majid Naderi,* Noreen Pervaiz,* Joao Rocha,† and Michael W. Anderson*

*Department of Chemistry, UMIST, P.O. Box 88, Manchester M60 1QD, United Kingdom; and †Department of Chemistry, University of Aveiro, 3800 Aveiro, Portugal

Received November 27, 1997; revised April 2, 1998; accepted April 18, 1998

The dehydrocyclisation of *n*-hexane to benzene has long been reported to be selectively catalysed by Pt-KL and other Pt impregnated basic zeolites. In this contribution, Pt-impregnated basic microporous titanosilicates ETS-10 and ETAS-10 are shown to catalyse this reaction with remarkably high selectivities. Although these two materials are topologically identical, their catalytic performance differs substantially. Pt-ETAS-10 is less active and less selective than Pt-ETS-10, whereas selectivities for benzene were found to increase considerably with temperature for both catalysts. The selectivity difference between Pt-ETS-10 and Pt-ETAS-10 is more pronounced at higher reaction temperatures. The differing catalytic behaviour of these materials is suggested to relate to their chemical nature and may be explained on grounds of acidity. Although ETS-10 and ETAS-10 materials exhibit the same acidity, Pt-ETAS-10 was found to be more acidic than Pt-ETS-10. The enhanced acidity of Pt-ETAS-10 is purported to be responsible for its low catalytic performance.

INTRODUCTION

The conversion of C_6–C_8 paraffins to aromatic hydrocarbons is of great significance in the petroleum industry. In conventional reforming, C_6–C_8 paraffins hydrocrack over acidic Pt/alumina rather than dehydrocyclise to aromatics. It has already been demonstrated that basic zeolites, impregnated with a controlled amount of Pt, catalyse reforming reactions yielding aromatic hydrocarbons as the main products (1–10). The absence of acidity in these systems leads to monofunctional reforming where hydrocracking reactions are not favoured. In *n*-hexane reforming, monofunctional catalysts are suggested to form benzene and methylcyclopentane via one-six and one-five ring closures, respectively, whereas they are unable to directly convert methylcyclopentane to benzene (4). Among the basic zeolite catalysts, Pt supported on zeolite L exhibits the highest activity and selectivity. The remarkable catalytic performance of zeolite L has been proposed to relate to the effect of cations on the Pt electronic state (11–13) as well as to the structural geometry (14–16) of this material.

ETS-10 (Engelhard titanosilicate structure 10) is potentially a very important new microporous inorganic titanosilicate framework material. The structure which was first synthesised by Engelhard (17, 18) and solved by Anderson *et al.* (19–21) consists of corner sharing octahedral titanium(IV) and tetrahedral silicon. ETS-10 is one of a small group of zeolite or zeotype materials which contain a three-dimensional 12-ring pore system. Owing to the high framework charge associated with the octahedral Ti, ETS-10 also has a very high cation exchange capacity. Every titanium in the framework has an associated two minus charge which gives ETS-10 a similar ion-exchange capacity to zeolite Y. The basic anhydrous formula of ETS-10 is $M_{2/m}TiSi_5O_{13}^{m+}$ where M is a cation of charge m (3/2 Na^+ and 1/2 K^+ in the as-synthesised sample). Further interest resides in the fact that, like zeolite beta, ETS-10 is highly disordered, being composed of a random intergrowth of two end-member polymorphs. Polymorph A belongs to a chiral space group and, like zeolite beta, possesses a spiral channel. Additionally, isomorphous substitution to incorporate both aluminium (22) and gallium (23) into ETS-10, thus producing ETAS-10 and ETGS-10, respectively (24), has been reported.

The vast interest in these inorganic solids with regard to catalysis results from their unique structural characteristics as well as their novel chemical composition, and a number of contributions have already reported on the catalytic properties of ETS-10 materials (25–30). In this preliminary investigation, the catalytic performance of basic Pt-ETS-10 and Pt-ETAS-10 in *n*-hexane reforming reactions is described. Both materials catalyse this reaction, yielding selectivities similar to that of Pt-KL zeolite. Furthermore, the rather distinctive architecture of these materials coupled with their well-defined chemistry may give us a better insight into the mechanistic pathways of reforming reactions over monofunctional catalytic systems.

EXPERIMENTAL

Sample Preparation

ETS-10 and ETAS-10 samples were synthesised according to the methods reported by Engelhard (17, 18). The potassium form of these solids was prepared by ion

0021-9517/98 $25.00

exchange of the as-synthesised materials with 0.1 *M* KNO_3 at 60°C. All these supports were impregnated with platinum using an aqueous solution of tetraammineplatinum(II) nitrate to weight loadings of ca 1.6–2.0%. The platinum-impregnated catalysts were calcined in air at 350°C for 5 h and the heating rate was 1°C min^{-1}. All these materials were fully characterised at different stages of the preparation as well as after the catalytic tests by powder XRD, ^{29}Si, ^{27}Al, and ^{1}H MAS NMR, N_2 adsorption measurements, electron dispersive analysis of X-rays (EDAX) and electron microscopy.

Catalysis

These experiments were performed in a fixed-bed stainless steel reactor at atmospheric pressure. The reactor's length and internal diameter are 16 and 0.5 cm, respectively, and the reactor bed measures 1 cm long and exhibits an internal diameter of 0.5 cm. The catalysts (50 mg) was reduced at 450°C in a hydrogen containing carrier gas (H_2 20% in Ar) with a flow rate of 10 ml min^{-1} and a heating rate of 3°C min^{-1} for 3 h. To assess the effect of the reaction temperature on this catalytic process, these experiments were carried out at two different reaction temperatures, 400 and 450°C. The reactant was fed and controlled by a syringe pump and the H_2/hexane molar ratio was kept constant at eight. Contact times were adjusted by keeping the catalyst volume constant and altering the volumetric flow rate of the reactant and were calculated at the reaction conditions on a volume basis. Products were analysed *in situ* using gas chromatography. These analyses were carried out isothermally at 45°C by means of a 30-m long capillary column (DP1 fused silica phase) and an FID (flame ionisation detector).

RESULTS AND DISCUSSION

Characterisation of Pt-ETS-10 and Pt-ETAS-10

The X-ray diffractograms of these materials were recorded at different stages of this experimental process in order to assess any crystallinity losses and structural distortions. Figure 1 shows the diffractograms of (a) as-synthesised, (b) Pt-impregnated and calcined, and (c) post-hydrogen reduction and catalytic test ETAS-10. These results clearly indicate that although loss of crystallinity is unavoidable, the ETAS-10 structure remains intact during this series of experiments. The sharp reflection appearing at $2\theta = 39.6°$ in the diffractogram of the Pt-ETAS-10 results from metallic Pt (with reference to *Join Committee on Powder Diffraction Standards*, Card No. 04-0802). The additional and rather strong reflection at $2\theta = 38°$ in the diffractogram of Pt-ETAS-10 recorded after the catalytic test, could be attributed to a Pt-hydrocarbon complex. These two Pt related reflections were also observed in the Pt-ETS-10 diffractograms, and the structure of Pt-ETS-10 was also intact after the catalytic tests.

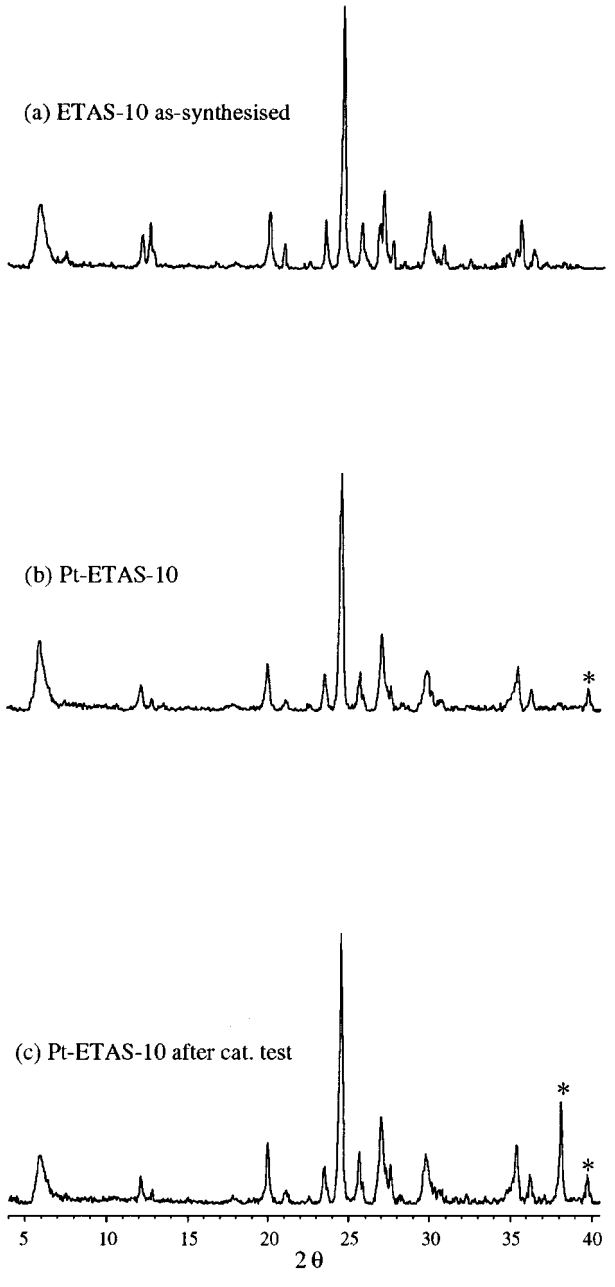

FIG. 1. Powder X-ray diffractograms of (a) as-synthesised ETAS-10, (b) Pt-impregnated and calcined Pt-ETAS-10, and (c) Pt-ETAS-10 after catalysis; Pt related reflections are denoted by asterisks.

Further characterisation was performed by means of ^{29}Si, ^{27}Al, and ^{1}H MAS NMR experiments on both, the as-synthesised form of these inorganic solids, as well as the Pt-impregnated materials. The ^{29}Si and ^{27}Al MAS NMR spectra of the as-synthesised ETS-10 and ETAS-10 samples (not shown), used in these experiments, are very similar to the corresponding spectra published earlier (19, 22, 24). Furthermore Pt-impregnation and calcination has little

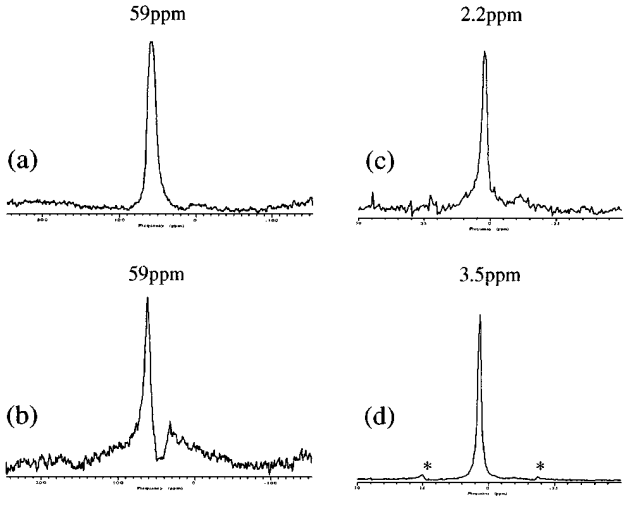

FIG. 2. (a) ^{27}Al MAS NMR spectrum of Pt-ETAS-10 recorded before reaction, (b) ^{27}Al MAS NMR spectrum of Pt-ETAS-10 recorded after reaction, (c) ^{1}H MAS NMR spectrum of Pt-ETS-10, (d) ^{1}H MAS NMR spectrum of Pt-ETAS-10; asterisks denote spinning sidebands.

effect on these spectra. Figures 2a and 2b show the ^{27}Al MAS NMR spectra of the Pt-ETAS-10 samples recorded before and after catalysis, respectively. The sample before catalysis has been Pt-impregnated and calcined and its spectrum depicts one line at 59 ppm assigned to framework tetrahedral aluminium. Conversely, the ^{27}Al MAS NMR spectrum of the Pt-ETAS-10 catalyst, recorded after the catalytic test, exhibits an additional featureless line covering the chemical shift range of −50 to 150 ppm. The broadness of this resonance, which accounts for 75% of the spectrum, is characteristic of second-order quadropolar effects which, in turn, are indicative of aluminium in a distorted environment. Extraframework aluminium in either six-coordinate hydrated form or in an amorphous aluminosilicate phase can be in a very distorted chemical environment and thus produce such a broad line shape. This experimental finding indicates that 75% of the framework aluminium dislodges from the lattice during the reforming reaction. Figures 2c and 2d show the ^{1}H MAS NMR spectra of Pt-impregnated and calcined ETS-10 and ETAS-10, respectively. The spectrum of Pt-ETS-10 (see Fig. 2c) exhibits one weak signal at 2.2 ppm assigned to terminal nonacidic protons. On the contrary, the ^{1}H MAS NMR spectrum of Pt-ETAS-10 (see Fig. 2d) depicts a strong signal at 3.5 ppm attributed to mildly acidic protons. Based on this spectroscopic evidence, Pt-ETAS-10 is suggested to be more acidic than Pt-ETS-10 and the enhanced acidity of Pt-ETAS-10 must relate to Pt impregnation.

Table 1 illustrates the main aspects of the chemical composition of these catalysts which was obtained by EDAX (electron dispersive analysis of X-rays) using electron microscopy. These experiments were performed on the Pt impregnated and calcined materials and Pt loadings of ca 1.6–2.0 w/w% were found for all these catalysts. Of great interest are the Na/K ratios in Pt-ETS-10 and Pt-ETAS-10. At this point it is worth noting that the as-synthesised ETS-10 comprises Na and K cations in a ratio of Na/K = 3, whereas the as-synthesised ETAS-10 accommodates more K cations than ETS-10. For the catalysts used in this investigation, the Pt-ETAS-10 sample was found to contain more than two times the amount of K accommodated in Pt-ETS-10. Furthermore, ion exchange to K form has yielded an increase in the K content by a factor of three for both samples.

Pt particles in the range of 40–70 nm were observed outside the channels of these Pt impregnated and calcined materials, by electron microscopy. However, the active centres are believed to be small electron-rich Pt clusters (2) inside the pores which could not be easily seen in these micrographs. Finally, N_2 adsorption experiments on all these materials yield isotherms of type I, characteristic of microporosity with maximum uptakes of ca 12–15 w/w%. Pt impregnation and calcination has no effect on the adsorption behaviour of these solids.

Catalytic Reactions of n-Hexane over Pt-ETS-10 and Pt-ETAS-10

The major reactions of *n*-hexane over both Pt-ETS-10 and Pt-ETAS-10 entail dehydrocyclisation to benzene and methylcyclopentane, skeletal isomerisation to methylpentanes and dimethylbutanes and hydrogenolysis to form C_1–C_5 paraffins. Conversions hereafter are calculated as the weight percent of *n*-hexane reacted and benzene selectivities are calculated by dividing the benzene yield by the *n*-hexane conversion. Aromatisation of *n*-hexane is catalysed by all Pt loaded catalysts used in this investigation, yielding very high selectivities for benzene. However, in the absence of Pt, these materials exhibit a very low catalytic activity with *n*-hexane conversion of less than 5 w/w%, producing mainly C_1–C_5 paraffins and olefins.

Catalytic Activity of Pt-ETS-10

The catalytic performance of Pt-ETS-10 is best described in Figs. 3–6. Figure 3 depicts the product distribution of *n*-hexane reaction over Pt-ETS-10 at 450°C and at

TABLE 1

The Main Aspects of the Chemical Composition of These Solids Obtained by EDAX

	Pt-ETS-10	Pt-ETAS-10	Pt-K-ETS-10	Pt-K-ETAS-10
Pt (w/w%)	1.8	1.6	1.9	2.0
Na/K (mol)	3.4	1.6	1.0	0.5
Al/Ti (mol)[a]	—	0.3	—	0.3

[a] Calculated using the ^{29}Si MAS NMR of these samples (22).

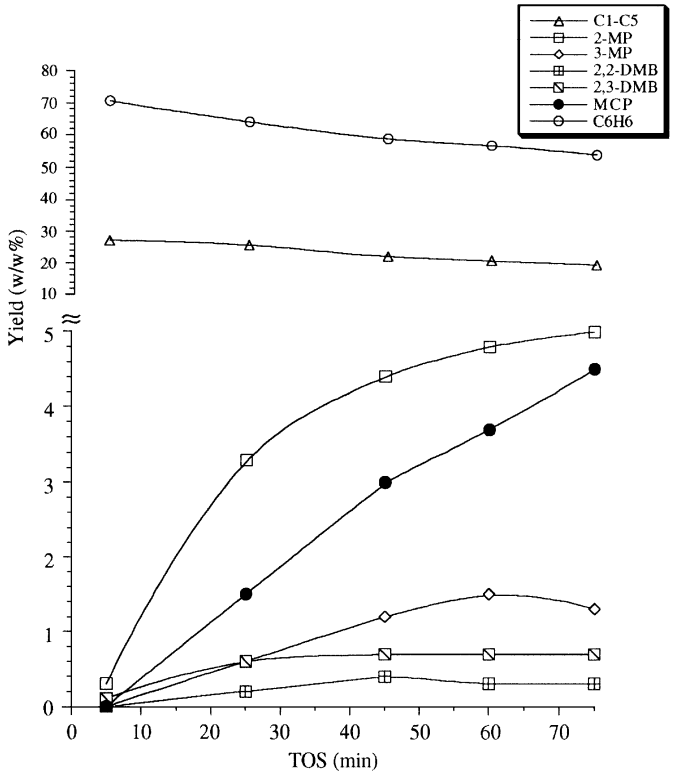

FIG. 3. The effect of TOS on the product distribution (w/w%) in *n*-hexane reforming reaction over Pt-ETS-10 at 450°C and with the contact time of 15 s. (C_1–C_5 = paraffinic hydrocarbons in this range; 2-MP = 2-methylpentane; 3-MP = 3-methylpentane; 2,2-DMB = 2,2-dimethylbutane; 2,3-DMB = 2,3-dimethylbutane; MCP = methylcyclopentane and C_6H_6 = benzene.)

different times on stream (TOS). It is clearly shown that *n*-hexane dehydrocyclisation and, thus, benzene formation dominates in this catalytic process at all TOS with benzene yields of up to 71 w/w%. The second main group of products is C_1–C_5 paraffins, resulting from hydrogenolysis reactions and accounting for about 25 w/w% of the product stream. Skeletal isomerisation is also observed at these conditions evidenced by the presence of 2- and 3-methylpentanes and to a lesser extent dimethylbutanes. Another interesting feature seen in this graph is the presence of methylcyclopentane and its dramatic increase with TOS. In addition, while the yields of benzene and C_1–C_5 decay very smoothly with TOS the amounts of isomerisation products tend to increase with TOS. This leads to a small decrease in selectivity for benzene at long TOS.

Figure 4 shows the product stream composition at 400°C and at various TOS. The pattern of products in this figure appears to be similar to that described above with benzene appearing as a dominant feature. Though isomerisation seems to be favoured at these conditions with 2- and 3-methylpentane reaching yields of ca 8 and 5 w/w%, respectively, dimethylbutanes were only detected in negligible quantities.

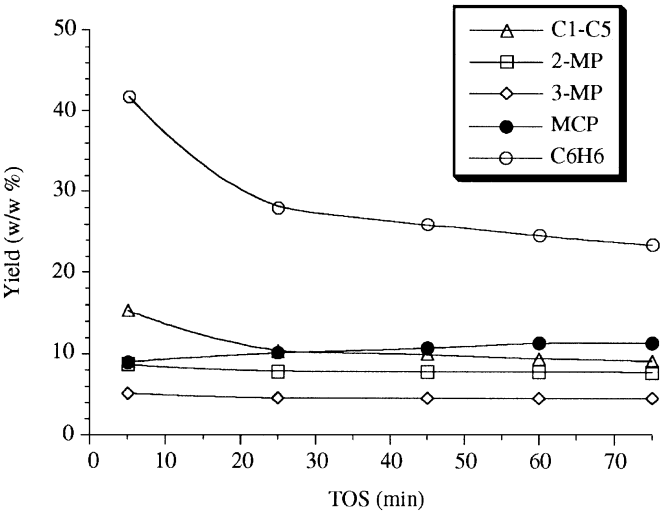

FIG. 4. The effect of TOS on the product distribution (w/w%) in *n*-hexane reforming reaction over Pt-ETS-10 at 400°C and with the contact time of 15 s. (C_1–C_5 = paraffinic hydrocarbons in this range; 2-MP = 2-methylpentane; 3-MP = 3-methylpentane; MCP = methylcyclopentane and C_6H_6 = benzene.)

Table 2 illustrates the product distribution of paraffinic hydrocarbons in the range of C_1–C_5 for Pt-ETS-10 at 400 and 450°C. A similar pattern was observed at both temperatures with pentane isomers being a dominant feature in this fraction of the product stream.

Figure 5 highlights the effect of temperature on conversions and selectivities of these materials at different TOS. High temperatures favour the endothermic dehydrocyclisation reactions at the expense of the exothermic isomerisation reactions which are in turn favoured at lower temperatures. As a result the selectivity for benzene increases markedly with temperature. As shown in this figure, at the temperature of 450°C benzene selectivities of ca 70 w/w% were achieved at conversion levels of ca 90 w/w%. These findings point to an excellent catalytic performance which may only be accomplished by a few members of the zeolite and zeotype family such as Pt-KL and Pt-NaY. Because dehydrocylisation reactions take place on Pt sites, the small decay in selectivities and rather more noticeable decrease in conversions with TOS is suggested to relate to Pt

TABLE 2

Product Distribution in the Range of C_1–C_5 for Pt-ETS-10 and Pt-ETAS-10 at 400 and 450°C (w/w%); TOS = 60 min CT = 15 s

	Pt-ETS-10 400°C	Pt-ETS-10 450°C	Pt-ETAS-10 400°C	Pt-ETAS-10 450°C
C_1	6.3	8.8	5.9	4.3
C_2	13.7	16.6	11.8	12.5
C_3	6.5	5.4	11.8	8.3
C_4	5.5	5.4	11.8	8.3
C_5	68.0	63.8	58.7	66.6

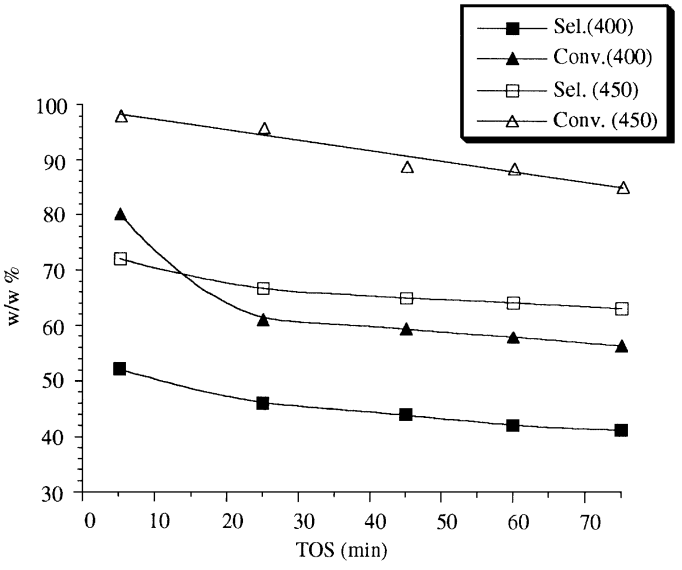

FIG. 5. The effect of TOS on conversions and selectivities for benzene in *n*-hexane reforming reaction over Pt-ETS-10 at 400 and 450°C with the contact time of 15 s. (Sel400 = selectivity for benzene at 400°C; Conv400 = conversion of *n*-hexane at 400°C; Sel450 = selectivity for benzene at 450°C; Conv450 = conversion of *n*-hexane at 450°C.)

deactivation. Pt deactivation has been proposed (6, 31) to result from a gradual replacement of the hydrogen in the active "Pt-H" site with partially dehydrogenated hydrocarbons and thus becomes "Pt-C-H." The last may dehydrogenate further to a "Pt-C" site and this fashion of deactivation has been found (6) to be more pronounced in the absence of acid sites.

Figure 6 shows the effect of contact time on conversions and selectivities in this catalytic process. At relatively short contact times in the range of 1–5 s, conversions vary in the region of 50–55 w/w% and the selectivities remain constant at ca 55 w/w%, whereas longer contact times enhance selectivies quite notably.

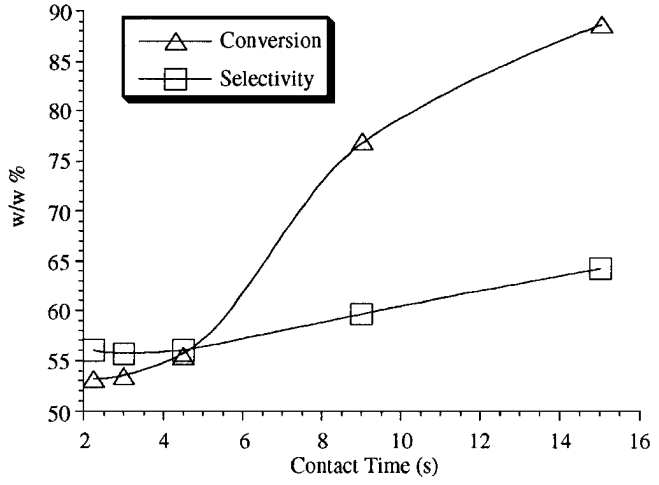

FIG. 6. The effect of contact time on conversion and selectivity in *n*-hexane reforming reaction over Pt-ETS-10 at 450°C and TOS = 60 min.

Catalytic Activity of Pt-ETAS-10

The catalytic performance of Pt-ETAS-10 is best described in Figs. 7–9. Figures 7 and 8 depict the product distribution of *n*-hexane reaction over Pt-ETAS-10 at 400 and 450°C, respectively. At both temperatures, *n*-hexane converts mainly to benzene and methylcyclopentane while the relative contribution of hydrogenolysis and isomerisation reactions is also quite profound. As a result, C_1–C_5 hydrocarbons and methylpentanes appear to form in relatively significant amounts.

Table 2 illustrates the product distribution of paraffinic hydrocarbons in the range of C_1–C_5 for Pt-ETAS-10 at 400 and 450°C. As observed with Pt-ETS-10, the reaction temperature has little effect on the product distribution in this hydrocarbon range.

Figure 9 illustrates the effect of temperature on conversions and selectivities at different TOS in this reaction process. As observed in the case of Pt-ETS-10 high temperatures favour benzene selectivities which remain constant

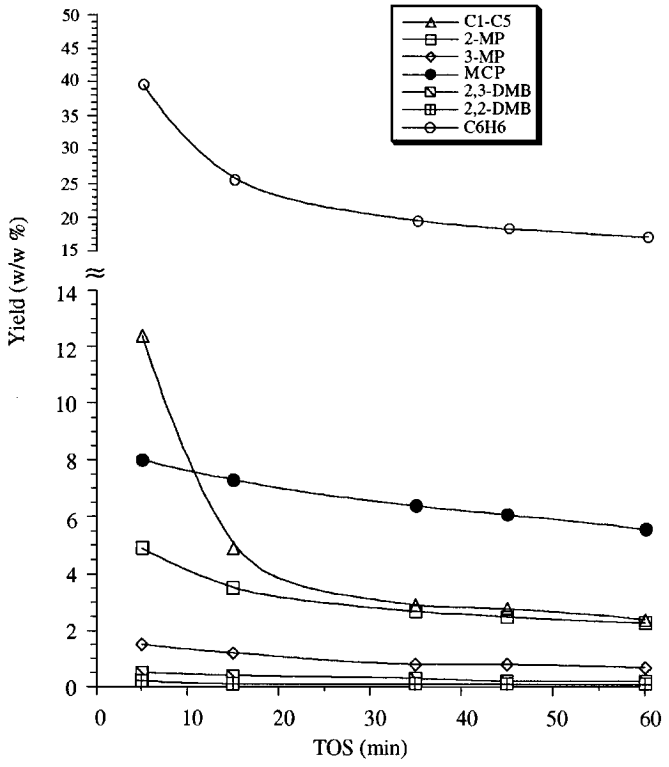

FIG. 7. The effect of TOS on the product distribution (w/w%) in *n*-hexane reforming reaction over Pt-ETAS-10 at 450°C and with the contact time of 15 s. (C_1–C_5 = paraffinic hydrocarbons in this range; 2-MP = 2-methylpentane; 3-MP = 3-methylpentane; 2,2-DMB = 2,2-dimethylbutane; 2,3-DMB = 2,3-dimethylbutane; MCP = methylcyclopentane and C_6H_6 = benzene.)

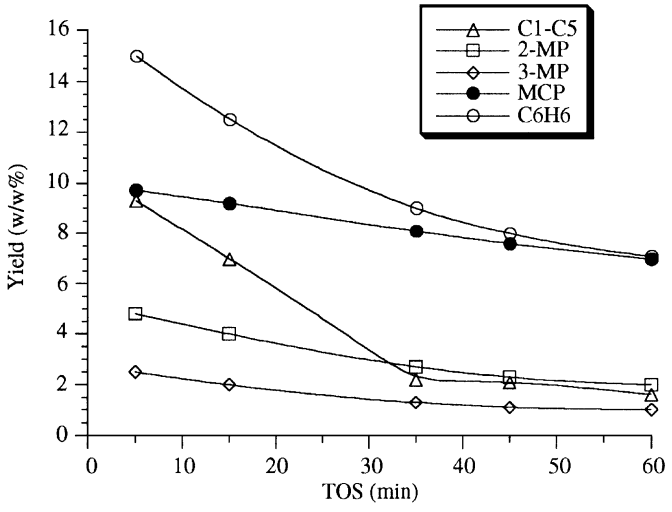

FIG. 8. The effect of TOS on the product distribution (w/w%) in *n*-hexane reforming reaction over Pt-ETAS-10 at 400°C and with the contact time of 15 s. (C_1–C_5 = paraffinic hydrocarbons in this range; 2-MP = 2-methylpentane; 3-MP = 3-methylpentane; MCP = methylcyclopentane and C_6H_6 = benzene.)

with TOS. Conversely, a striking decay in conversion with TOS is observed at both temperatures.

Comparison of Pt-ETS-10 and Pt-ETAS-10 Catalytic Activities

With reference to Figs. 3 and 5 one can clearly see that Pt-ETS-10 exhibits an excellent catalytic performance reaching selectivities of ca 70 w/w% and conversion levels of ca 90 w/w% at 450°C. The activity and selectivity of this material appears to be comparable to those of Pt-KL and Pt-NaY which are considered to be excellent catalysts for this reaction. Pt-ETAS-10 is less active than Pt-ETS-10 at both reaction temperatures, 400 and 450°C. Although, both materials exhibit very similar selectivities at 400°C (ca 40 w/w% at TOS = 60 min), Pt-ETAS-10 was found to be less selective at 450°C with selectivities hardly reaching 60 w/w%. Furthermore, Pt-ETS-10 deactivates much slower than Pt-ETAS-10, whereas a small decay in selectivity with TOS was observed for Pt-ETS-10. Owing to the fact that these two catalysts are topologically identical, the different catalytic activity can only be accounted for by differences in the chemical nature of these materials. Though Al is known to increase basicity in zeolitic materials (32), it can be argued that the low selectivity of Pt-ETAS-10 may be due to the acidity induced by Al incorporation in to the ETS-10 lattice. However, the acidity of ETAS-10 in both, as-synthesised and proton form is very weak (28) and very similar to that of ETS-10. ^{1}H MAS NMR spectra of the as-synthesised ETS-10 and ETAS-10 materials show very similar peak patterns in the range of 1–2.5 ppm assigned to terminal nonacidic protons. Furthermore, the ^{27}Al MAS NMR spectrum (22) of ETAS-10 illustrates that the amount of extraframework Al, which could potentially generate Lewis acidity, is seemingly negligible. Although the acidity of ETS-10 and ETAS-10 is literally identical, Pt-ETAS-10 is found to be more acidic than Pt-ETS-10. With reference to Figs. 2c and 2d, one may conclude that Pt impregnation and calcination has enhanced the acidity of ETAS-10, whereas Pt-ETS-10 maintains the same weak acidity as the support ETS-10. Further evidence as to the raised acidity of Pt-ETAS-10 catalyst rest with the ^{27}Al MAS NMR spectra of this material. As stated in the characterisation section and shown in Fig. 2a, Pt impregnation and calcination had no effect on the ^{27}Al MAS NMR spectrum of this material. However, the ^{27}Al MAS NMR spectrum of the Pt-ETAS-10 recorded after catalysis indicates that 75% of the framework aluminium dislodges from the lattice during the reforming reaction. There are two possibilities for the location of extraframework Al: (i) amorphous aluminosilicate; (ii) six-coordinate, hydrated aluminium. In view of the reduced crystallinity, the former seems more likely. However, either form would enhance the overall acidity of the Pt-ETAS-10 catalysts.

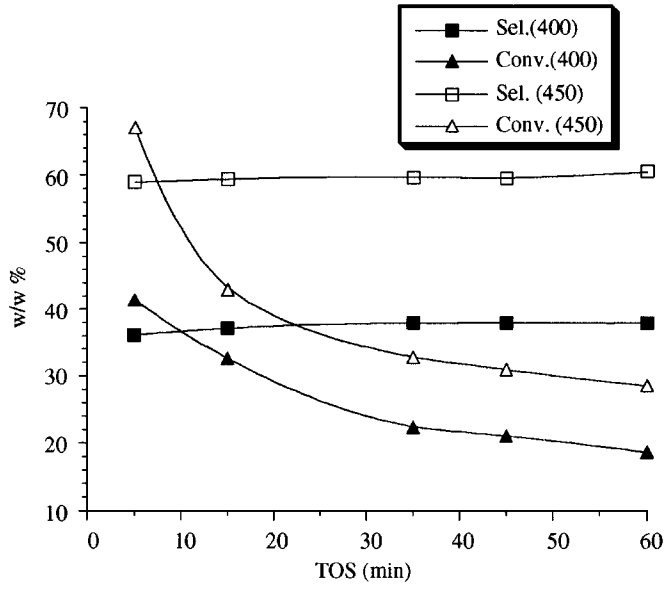

FIG. 9. The effect of TOS on conversions and selectivities for benzene in *n*-hexane reforming reaction over Pt-ETAS-10 at 400 and 450°C with the contact time of 15 s. (Sel400 = selectivity for benzene at 400°C; Conv400 = conversion of *n*-hexane at 400°C; Sel450 = selectivity for benzene at 450°C; Conv450 = conversion of *n*-hexane at 450°C.)

The high catalytic activity and selectivity of Pt impregnated basic zeolites has been suggested to relate to their basicity and thus to their ability to donate electrons to Pt active sites (11–13). Hence, high basicity implies high catalytic activity and selectivity for this reaction. Therefore, the low catalytic activity of Pt-ETAS-10 is purported to relate to the enhanced acidity of this material which in turn reduces the electron density of the Pt active sites. In addition, the extraframework aluminium and the formation

TABLE 3

The Effect of K Cations on the Catalytic Performance

	Pt-ETS-10	Pt-K-ETS-10	Pt-ETAS-10	Pt-K-ETAS-10
Conversion (w/w%)	58.1	23.1	18.7	25.3
Selectivity (w/w%)	42.3	35.5	38.0	39.5

Note. TOS = 60 min; CT = 15 s; $T = 400^{\circ}$C.

of an amorphous phase could physically reduce the accessibility to Pt active sites and this would explain both the low conversion and the fast deactivation of this material. Furthermore, the acid function of Pt-ETAS-10 is seemingly obvious at higher reaction temperatures and as a result the selectivity difference between Pt-ETS-10 and Pt-ETAS-10 becomes more pronounced.

Catalytic Activity of Pt-K-ETS-10 and Pt-K-ETAS-10

As mentioned above the basicity of framework aluminosilicate materials may be enhanced by increasing the Al content. Alternatively, ion exchange to larger monovalent cations may also increase the basicity of a zeolitic material (32). For example, ion exchange of Na-X to K-X or Cs-X leads to a dramatic increase in basicity of this material. The role of the alkali metal size in reforming reactions is yet not very clear. Ion exchange of NaL to KL or RbL has reported (1, 2) to enhance the catalytic activity of these materials, whereas ion exchange of Na-Y to Cs-Y has the opposite effect (5).

Table 3 depicts the catalytic activity of Pt-K-ETS-10 and Pt-K-ETAS-10, in comparison with that of Pt-ETS-10 and Pt-ETAS-10. The ion exchange of Pt-ETAS-10 to the K form does not significantly influence the catalytic performance of this solid. Conversely, the ion exchange of Pt-ETS-10 to the K form decreases dramatically the conversion level whilst has little effect on the selectivity of this catalyst. This rather controversial effect of K cations on the reforming catalysis of these two materials raises a number of questions. Both, steric and electrostatic interactions have to be deeply scrutinised in order to understand this fascinating catalytic behaviour of these materials. Basic site strength and distribution, alkali cations sittings, Pt particles size and distribution, and the acidity induced by Pt are the main factors that dictate the catalytic performance of these solids. Further work along this line is being carried out in order to gain a better insight of these novel inorganic catalysts.

CONCLUSION

Both, Pt-ETS-10 and Pt-ETAS-10 catalyse *n*-hexane reforming reactions, yielding high selectivities for benzene. Pt-ETS-10 exhibits an excellent catalytic performance with its activity and selectivity being comparable to those of Pt-KL and Pt-NaY. Pt-ETAS-10 is less active and less selective than Pt-ETS-10. The selectivity difference between Pt-ETS-10 and Pt-ETAS-10 is more pronounced at higher reaction temperatures. The lower catalytic activity of Pt-ETAS-10 can be explained on grounds of acidity. Although ETS-10 and ETAS-10 materials exhibit the same acidity, Pt-ETAS-10 was found to be more acidic than Pt-ETS-10. The enhanced acidity of Pt-ETAS-10 reduces the electron density of the Pt active sites to which accessibility may also be physically decreased by the formation of an amorphous aluminosilicate phase. This explains both the low conversion and the fast deactivation of Pt-ETAS-10.

ACKNOWLEDGMENTS

We thank Professor K. C. Waugh and Mr. P. Marenne at UMIST for our discussions on the Pt surface area and dispersion.

REFERENCES

1. Bernard, J. R., *in* "Proceedings 5th International Zeolite Conference" (L. V. C. Rees, Eds.), p. 686. Heyden, London, 1980.
2. Besoukhanova, C., Guidot, J., Barthomeuf, D., Breysse, M., and Bernard, J. R., *J. Chem. Soc. Faraday Trans. I* **77**, 1595 (1981).
3. Davis, R. J., and Derouane, E. G., *Nature* **349**, 313 (1991).
4. Lane, G. S., Modica, F. S., and Miller, J. T., *J. Catal.* **129**, 145 (1991).
5. Mielczarski, E., Hong, S. B., Davis, R. J., and Davis, M. E., *J. Catal.* **134**, 359 (1992).
6. Zhan, Z., Manninger, I., Paal, Z., and Barthomeuf, D., *J. Catal.* **147**, 333 (1994).
7. Davis, R., *Heterogeneous Chem. Rev.* **1**, 41 (1994).
8. Ivanova, I. I., Seirvert, M., Pasau-Claerbout, A., Blom, N., and Derouane, E. G., *J. Catal.* **164**, 347 (1996).
9. Ivanova, I. I., Pasau-Claerbout, A., Seirvert, M., Blom, N., and Derouane, E. G., *J. Catal.* **158**, 521 (1996).
10. Barthomeuf, D., *Catal. Rev.-Sci. Eng.* **38**(4), 521 (1996).
11. Besoukhanova, C., Breysse, M., Bernard, J. R., and Barthomeuf, D., *Stud. Surf. Sci. Catal.* **6**, 201 (1980).
12. Besoukhanova, C., Breysse, M., Bernard, J. R., and Barthomeuf, D., *in* "Proceedings, 7th International Congress on Catalysis," Vol. B, p. 1410. Elsevier, Amsterdam, 1980.
13. Larsen, G., and Haller, G. L., *Catal. Lett.* **3**, 103 (1989).
14. Derouane, E. G., and Vanderveken, D. J., *Appl. Catal.* **45**, 11 (1988).
15. Alvarez, W. E., and Resasco, D. E., *Catal. Lett.* **8**, 53 (1991).
16. Gao, Z., Jiang, X., Ruan, Z., and Xu, Y., *Catal. Lett.* **19**, 81 (1993).
17. Kuznicki, S. M., U.S. Patent 4,853,202 (1989).
18. Kuznicki, S. M., and Thrush, K. A., Europ. Patent 0405978A1 (1990).
19. Anderson, M. W., Terasaki, O., Ohsuna, T., Philippou, A., MacKay, S. P., Ferreira, A., Rocha, J., and Lidin, S., *Nature* **367**, 347 (1994).
20. Ohsuna, T., Terasaki, O., Watanabe, D., Anderson, M. W., and Lidin, S., *in* "Zeolites and Related Microporous Materials: State of the Art 1994, Stud. Surf. Sci. Catal." (J. Weitkamp, H. G., Karge, H. Pfeifer, and W. Hölderich, Eds.), Vol. 84, p. 413. Elsevier, Amsterdam, 1994.
21. Anderson, M. W., Terasaki, O., Ohsuna, T., O'Malley, P. J., Philippou, A., MacKay, S. P., Ferreira, A., Rocha, J., and Lidin, S., *Phil. Mag.* **71**, 813 (1995).
22. Anderson, M. W., Philippou, A., Lin, Z., Ferreira, A., and Rocha, J., *Angew. Chem. Int. Ed. Engl.* **34**, 1003 (1995).

23. Rocha, J., Lin, Z., Ferreira, A., and Anderson, M. W., *J. Chem. Soc., Chem. Commun.* **8**, 867 (1995).
24. Anderson, M. W., Rocha, J., Lin, Z., Philippou, A., Orion, I., and Ferreira, A., *Micropor. Mater.* **6**, 195 (1996).
25. Das, T. K., Chandwadkar, A. J., and Sivasanker, S., *Bull. Mat. Sci.* **17**, 1143 (1994).
26. Robert, R., Rajamohanan, S. G., Hegde, S. G., Chandwadkar, A. J., and Ratnasamy, P., *J. Catal.* **155**, 345 (1995).
27. Das, T. K., Chandwadkar, A. J., and Sivasanker, S., *J. Mol. Catal. A-Chemical* **107**, 199 (1996).
28. Liepold, A., Roos, K., Reschetilowski, W., Lin, Z., Rocha, J., Philippou, A., and Anderson, M. W., *Micropor. Mat.* **10**, 211 (1997).
29. Das, T. K., Chandwadkar, A. J., Soni, H. S., and Sivasanker, S., *Catal. Lett.* **44**, 113 (1997).
30. Deeba, M., Keweshan, C. F., Koermer, G. S., Kusnicki, S. M., and Madon, R. S., *Chem. Indus. Ser.* **53**, 383 (1994).
31. Sárkány, A., *J. Chem. Soc. Faraday Trans. I* **85**, 1523 (1989).
32. Barthomeuf, D., and de Mallmann, A., *in* "Innovation in Zeolite Materials Science" (P. J. Grobet, W. J. Mortier, E. F. Vansant, and G. Schulz-Ekloff, Eds.), p. 365. Elsevier, Amsterdam, 1988.